

Supporting Information

CFA-4 - a fluorinated metal-organic framework with exchangeable interchannel cations

Julia Fritzsche,^a Maciej Grzywa,^a Dmytro Denysenko,^a V. Bon,^b Irena Senkovska,^b Stefan Kaskel,^b and Dirk Volkmer ^{*a}

^a Institute of Physics, Chair of Solid State and Materials Chemistry, Augsburg University, Universitätsstrasse 1, 86159 Augsburg, Germany

^b Department of Inorganic Chemistry, Dresden University of Technology, Bergstrasse 66, 01062 Dresden, Germany

Contents:

1.	Crystallographic data and topology analysis	S2
2.	NMR spectra	S6
3.	IR spectra	S9
4.	(Variable Temperature) X-Ray Powder Diffraction Pattern	S11
5.	TGA curve	S13
6.	Mass spectra	S14
7.	EDX data	S16
8.	Gas sorption measurements	S17
9.	UV-Vis spectrum	S23
10.	Photoluminescence spectra	S24

* Corresponding author. Fax: +49 (0)821 598–5955; Tel: +49 (0)821 598–3006; E-mail:
dirk.volkmmer@physik.uni-augsburg.de

1. Single Crystal Structure Analysis of 1,4-bis(3,5-bis(trifluoromethyl)-1*H*-pyrazole-4-yl)benzene ·2MeOH ($C_{16}H_6F_{12}N_4 \cdot 2CH_3OH$).

1·2MeOH crystallizes in the monoclinic crystal system within the space group $C2/m$ (no. 12). The asymmetric unit consists of one nitrogen, six carbon, three fluoride, one oxygen and six hydrogen atoms accounting for 1/3 of $H_2\text{-tfpb}$ and one MeOH molecule. An Ortep-style plot of the asymmetric unit of **1·2MeOH** is shown in Fig. S1. While the $(CF_3)_2$ -pyrazole rings of the $H_2\text{-tfpb}$ molecule are almost parallel to the (100) plane, the phenyl ring is inclined with respect to the $(CF_3)_2$ -pyrazole rings. The two equatorial planes created by atoms belonging to the $(CF_3)_2$ -pyrazole rings and atoms of the phenyl ring enclose an angle of $57.44(5)$ °. The O1 and C6 atoms of MeOH are placed on a crystallographic mirror plane (4i in Wyckoff notation).

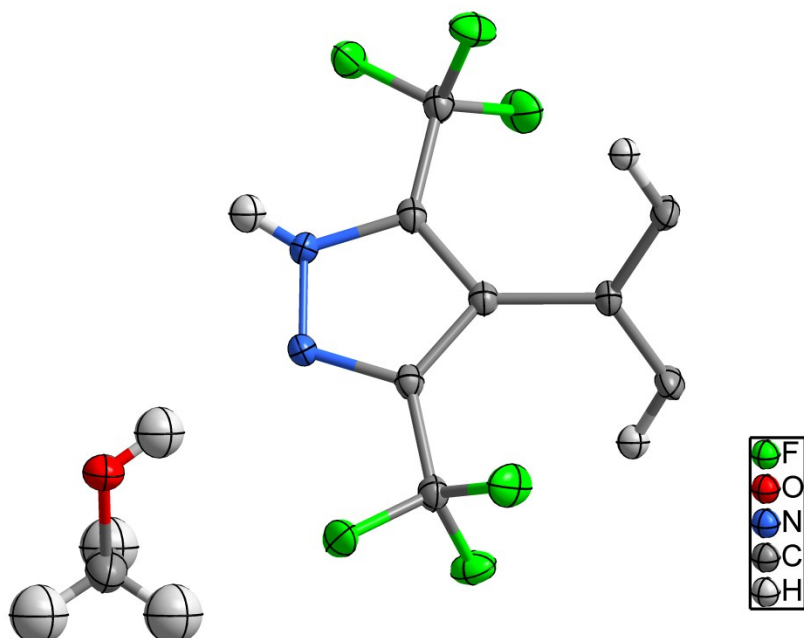


Fig. S1 Ortep-style plot of the asymmetric unit of **1·2MeOH**. Thermal ellipsoids probability: 50 %.

Compound **1** exhibits layered packing motif. Looking along the a -direction, the layers created by $H_2\text{-tfpb}$ molecules are separated by solvent molecules. The whole structure is stabilized by hydrogen bridges formed between MeOH molecules and nitrogen atoms of $H_2\text{-tfpb}$. List of the hydrogen bonds for **1·2MeOH** is presented in Table S1. The packing diagram of **1·2MeOH** along the a -direction is shown in Fig. S2.

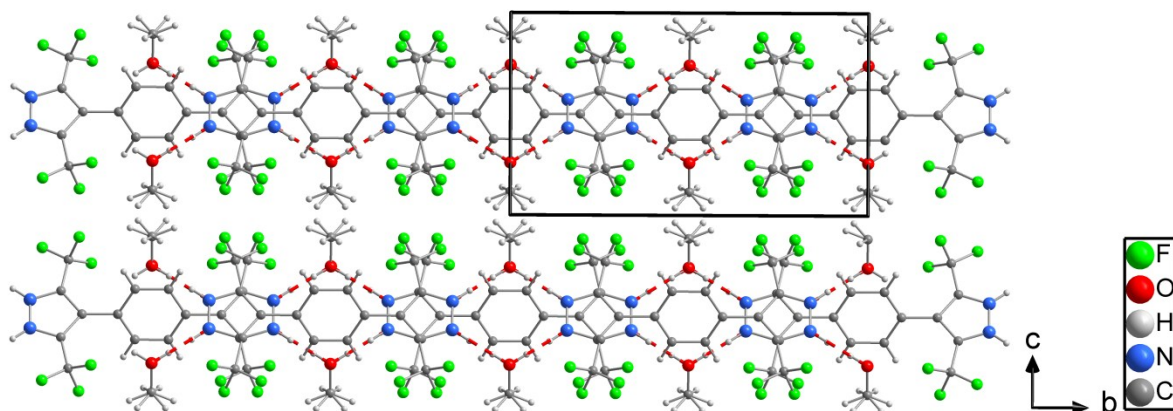


Fig. S2 Packing diagram of **1·2MeOH** with hydrogen bonds shown as intercepted red lines. Hydrogen atoms from $\text{H}_2\text{-tfpb}$ molecules are shown with 50 % occupation. (In the crystal structure of **1·2MeOH** the acidic NH-protons of the $\text{H}_2\text{-tfpb}$ molecule have been placed in calculated positions ($d(\text{NH}) = 0.88 \text{ \AA}$). Owing to lattice symmetry both nitrogen atoms of each pyrazole ring and oxygen atoms of MeOH molecules appear to be protonated at 50% probability).

Table S1 Hydrogen bonds for **1·2MeOH**

Donor---Hydrogen...Acceptor	Don--Hyd [Å]	Hyd--Acc [Å]	Don--Acc [Å]	D--H-----A
O1---H1...N1»1	0.84	1.95	2.782	173.7°
N1---H1A...O1	0.88	1.92	2.782	165.1°
O1---H1»1...N1	0.84	1.95	2.782	173.7°
N1»1---H1A»1...O1	0.88	1.92	2.782	165.1°
O1»2---H1»2...N1»4	0.84	1.95	2.782	173.7°
N1»2---H1A»2...O1»2	0.88	1.92	2.782	165.1°
O1»3---H1»3...N1»7	0.84	1.95	2.782	173.7°
N1»3---H1A»3...O1»3	0.88	1.92	2.782	165.1°
O1»2---H1»4...N1»2	0.84	1.95	2.782	173.7°
N1»4---H1A»4...O1»2	0.88	1.92	2.782	165.1°
N1»5---H1A»5...O1»5	0.88	1.92	2.782	165.1°
N1»6---H1A»6...O1»6	0.88	1.92	2.782	165.1°
O1»3---H1»7...N1»3	0.84	1.95	2.782	173.7°
N1»7---H1A»7...O1»3	0.88	1.92	2.782	165.1°

Topology analysis for Cu(I)[CFA-4]

Topology for Sc1

Atom Sc1 links by bridge ligands and has

Common vertex with R(A-A)					
V 1	0.3333	0.6667	0.5828	(0 0 0)	7.624A
Ti 1	0.6667	0.3333	0.7500	(0 0 0)	7.679A

Topology for Sc2

Atom Sc2 links by bridge ligands and has

Common vertex with R(A-A)					
V 1	-0.3333	0.3333	0.4172	(0 1 1)	7.702A
V 1	0.3333	0.6667	0.5828	(0 0 0)	7.702A

Topology for Ti1

Atom Ti1 links by bridge ligands and has

Common vertex with R(A-A)					
Sc 1	1.0002	0.4916	0.6651	(1 1 0)	7.679A
Sc 1	1.0002	0.5086	0.8349	(1 0 1)	7.679A
Sc 1	0.4914	0.4916	0.8349	(1 1 1)	7.679A
Sc 1	0.5084	-0.0002	0.8349	(0 0 1)	7.679A
Sc 1	0.4914	-0.0002	0.6651	(1 0 0)	7.679A
Sc 1	0.5084	0.5086	0.6651	(0 0 0)	7.679A

Topology for V1

Atom V1 links by bridge ligands and has

Common vertex with R(A-A)					
Sc 1	0.4914	0.9998	0.6651	(1 1 0)	7.624A
Sc 1	0.5084	0.5086	0.6651	(0 0 0)	7.624A
Sc 1	0.0002	0.4916	0.6651	(0 1 0)	7.624A
Sc 2	0.4569	1.0000	0.5000	(0 1 0)	7.702A
Sc 2	0.5431	0.5431	0.5000	(1 1 0)	7.702A
Sc 2	0.0000	0.4569	0.5000	(0 0 0)	7.702A

Structural group analysis

Structural group No 1

Structure consists of 3D framework with V2TiSc9

Coordination sequences

Sc1: 1 2 3 4 5 6 7 8 9 10
Num 2 10 10 46 30 120 54 210 94 330
Cum 3 13 23 69 99 219 273 483 577 907

Sc2: 1 2 3 4 5 6 7 8 9 10
Num 2 10 10 46 30 120 54 210 94 330
Cum 3 13 23 69 99 219 273 483 577 907

Ti1: 1 2 3 4 5 6 7 8 9 10
Num 6 6 30 20 90 42 162 74 282 114
Cum 7 13 43 63 153 195 357 431 713 827

V1: 1 2 3 4 5 6 7 8 9 10
Num 6 6 30 20 90 42 162 74 282 114
Cum 7 13 43 63 153 195 357 431 713 827

TD10=887

Vertex symbols for selected sublattice

Sc1 Point symbol:{8}

Sc1 Point symbol with loops:{4}

Extended point symbol:[8(4)]

Sc2 Point symbol:{8}

Sc2 Point symbol with loops:{4}

Extended point symbol:[8(4)]

Ti1 Point symbol:{8^9.12^6}

Ti1 Point symbol with loops:{4^9.6^6}

Extended point symbol:[8.8.8.8.8.8(2).8(2).8(2).12(8).12(8).12(8).12(8).12(8).12(8)]

V1 Point symbol:{8^9.12^6}

V1 Point symbol with loops:{4^9.6^6}

Extended point symbol:[8.8.8.8.8.8(2).8(2).8(2).12(8).12(8).12(8).12(8).12(8).12(8)]

Point symbol for net: {8^9.12^6}{8}3

Point symbol for net with loops: {4^9.6^6}{4}3

2,6-c net with stoichiometry (2-c)3(6-c); 2-nodal net

New topology

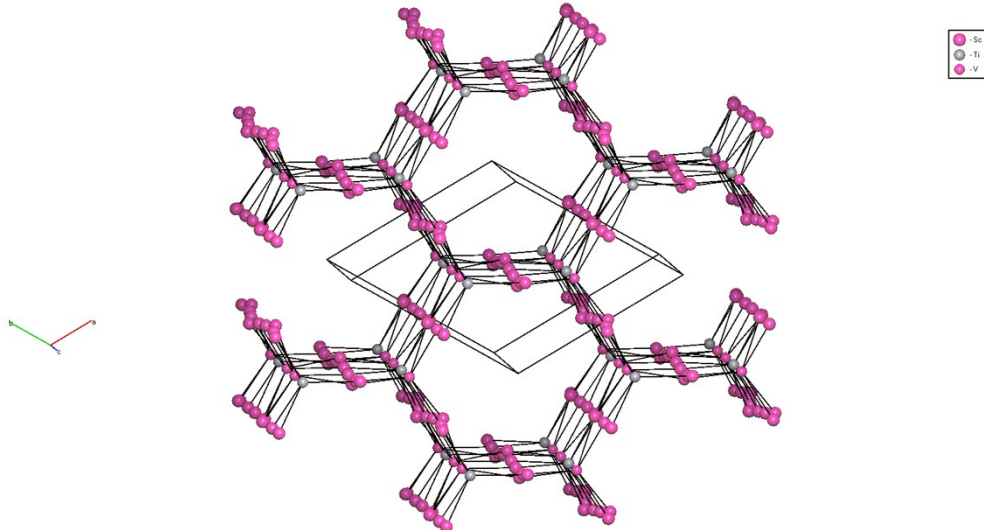


Fig. S3 Topological representation of Cu(I)[CFA-4].

2. NMR spectra of 1,4-bis(3,5-bis(trifluoromethyl)-1*H*-pyrazole-4-yl)benzene ($\text{H}_2\text{-tfpb}$)

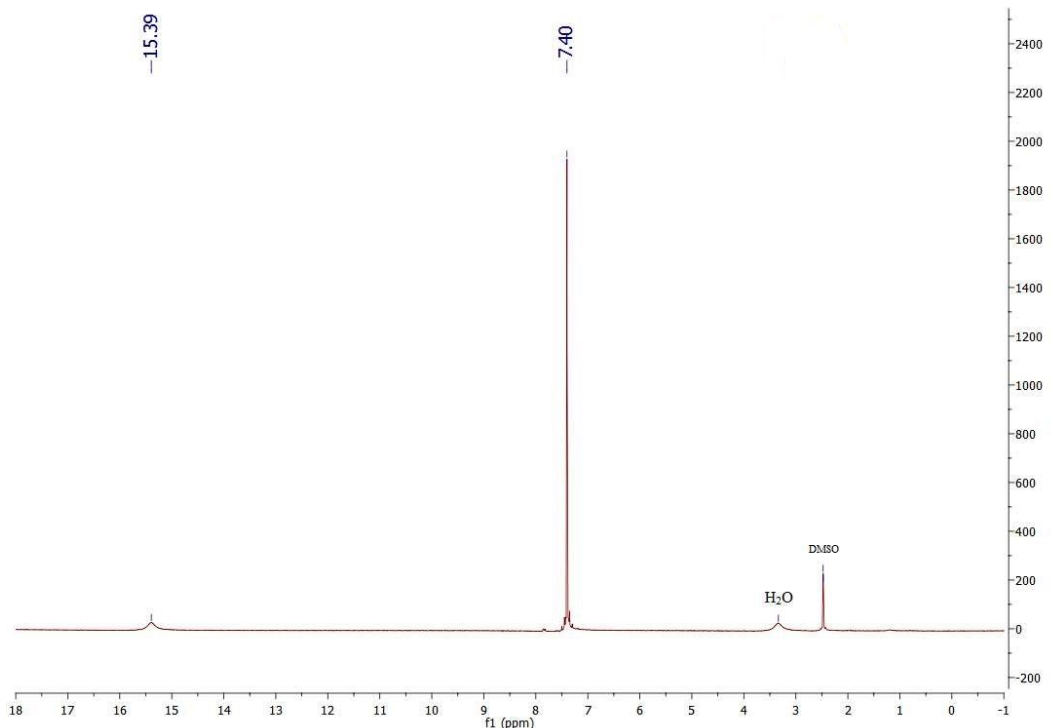


Fig. S4 ^1H -NMR spectrum of $\text{H}_2\text{-tfpb}$ in DMSO-d_6 .

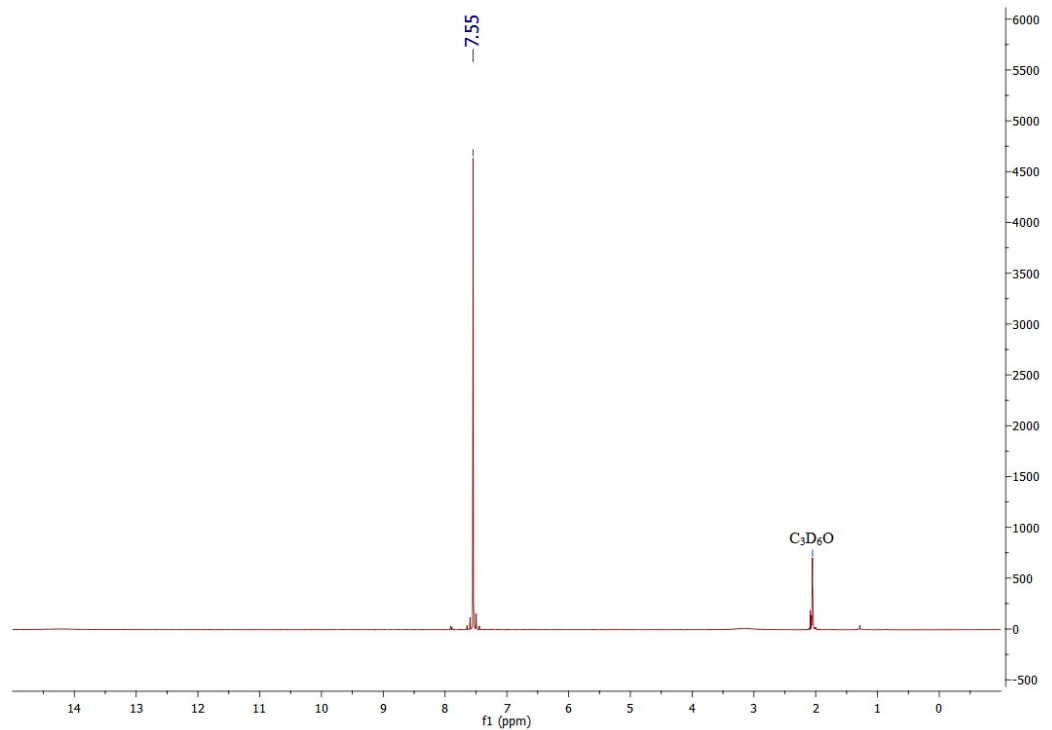


Fig. S5 ^1H -NMR spectrum of $\text{H}_2\text{-tfpb}$ in acetone-d_6 .

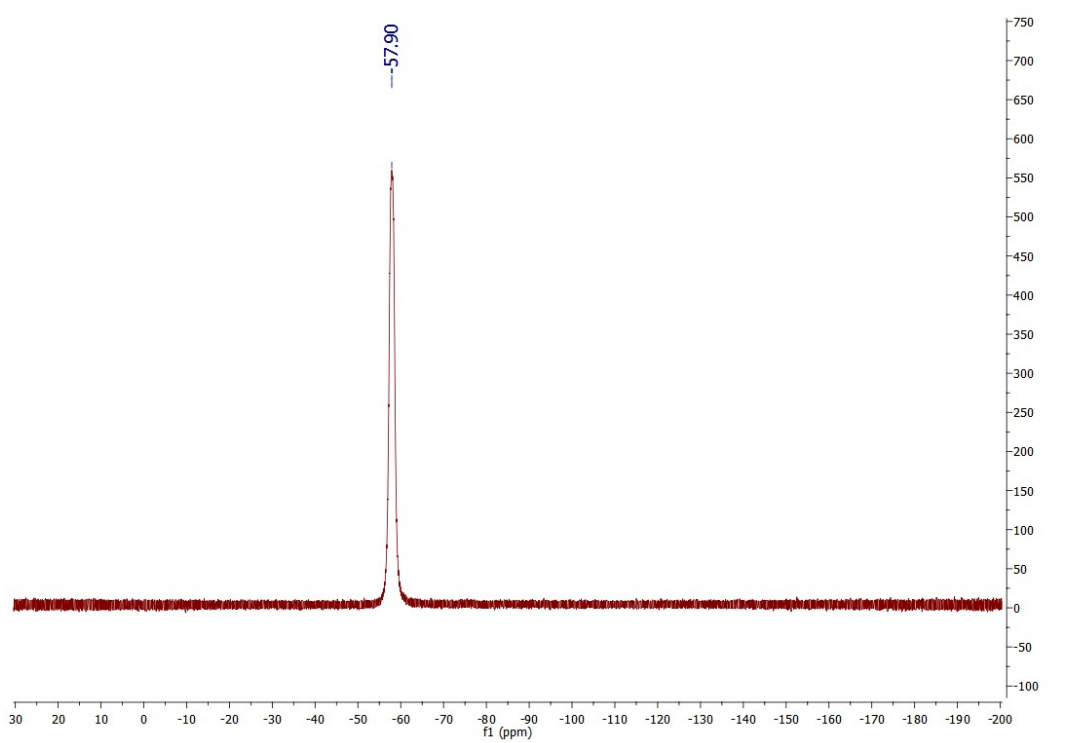


Fig. S6 ${}^{19}\text{F}$ -NMR spectrum of $\text{H}_2\text{-tfpb}$ in DMSO-d_6 .

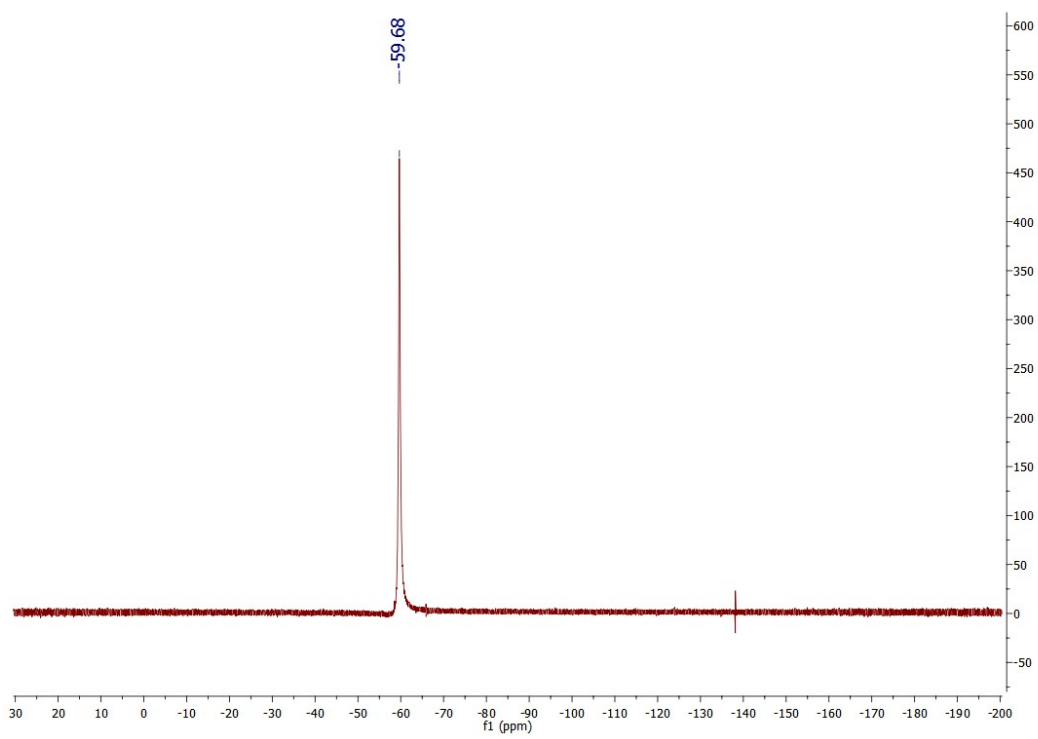


Fig. S7 ^{19}F -NMR spectrum of $\text{H}_2\text{-tfpb}$ in acetone- d_6 .

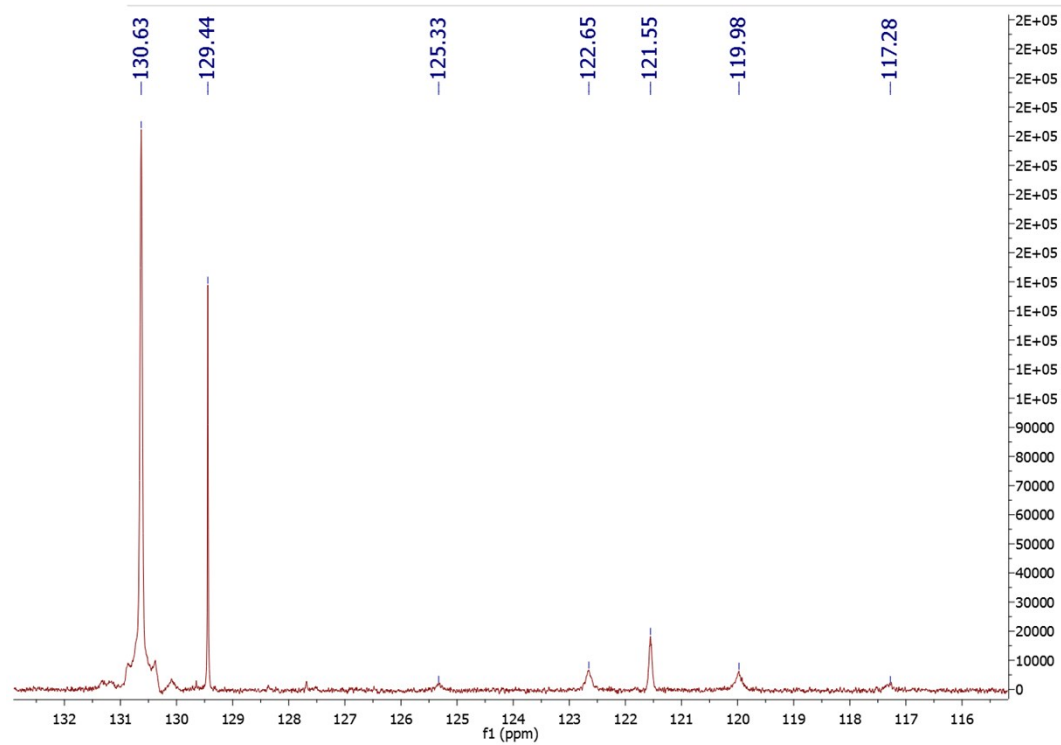


Fig. S8 ^{13}C -NMR spectrum of $\text{H}_2\text{-tfpb}$ in acetone- d_6 .

3. IR- Spectra

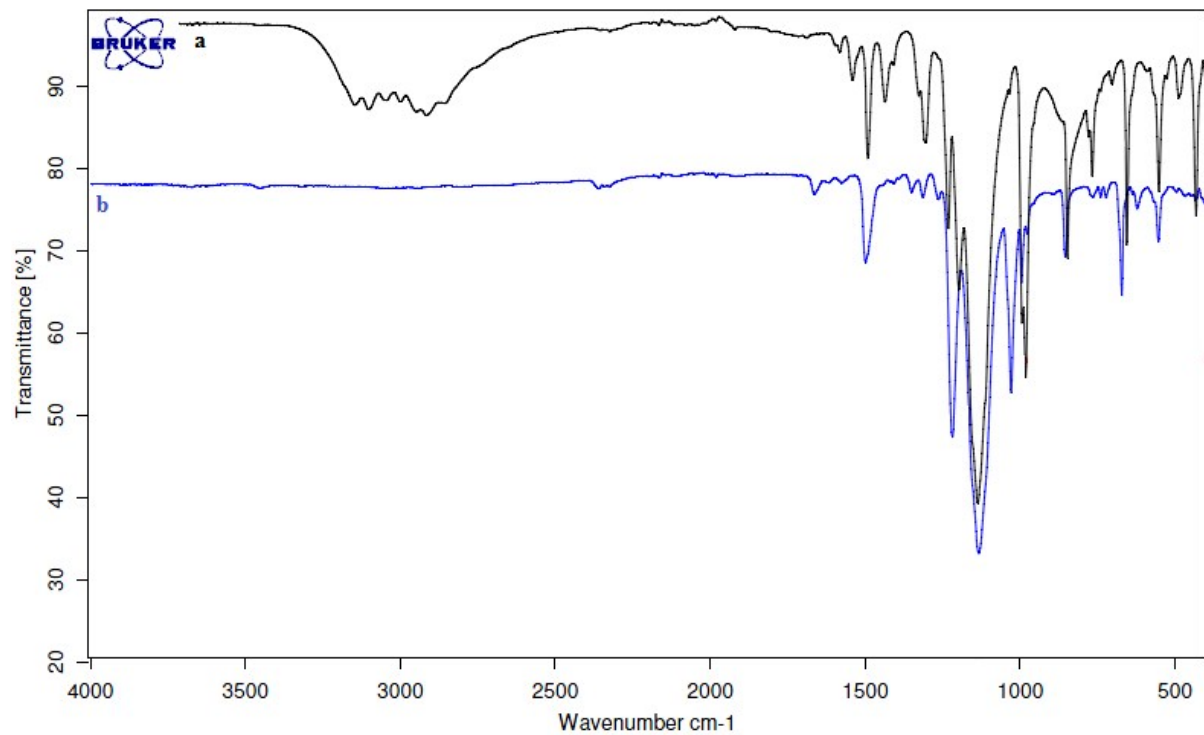


Fig. S9 Full-range IR spectra of a) $\text{H}_2\text{-tfpb}$; b) Cu(I)[CFA-4] .

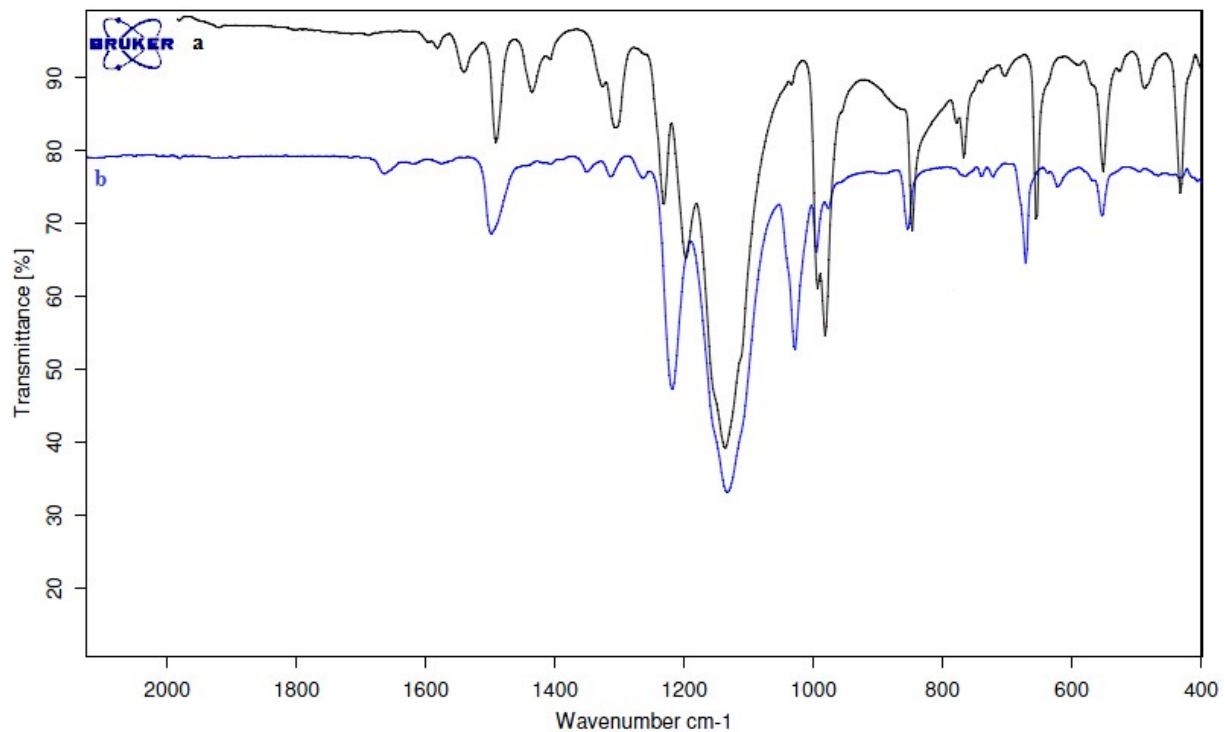


Fig. S10 IR spectra in the range $2000\text{-}400 \text{ cm}^{-1}$ of a) $\text{H}_2\text{-tfpb}$; b) Cu(I)[CFA-4] .

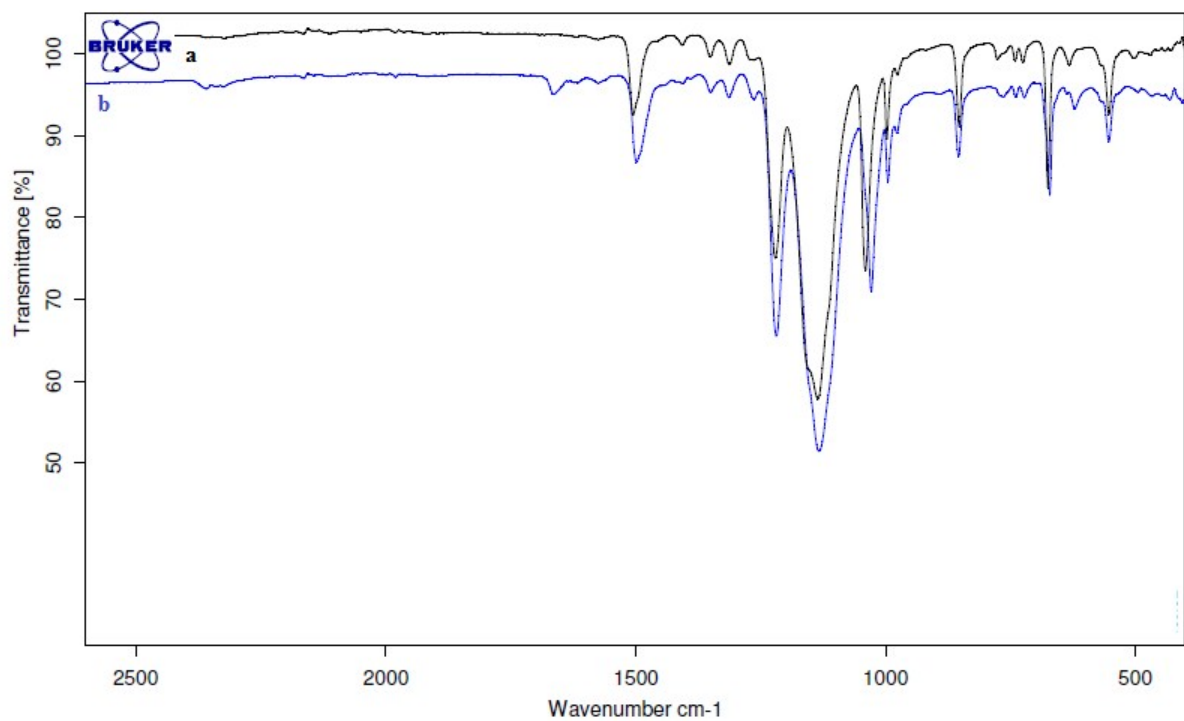


Fig. S11 IR spectra of **Cu(I)[CFA-4]**: a) after drying at 300°C; b) fresh sample.

4. X-Ray Powder Diffraction Pattern

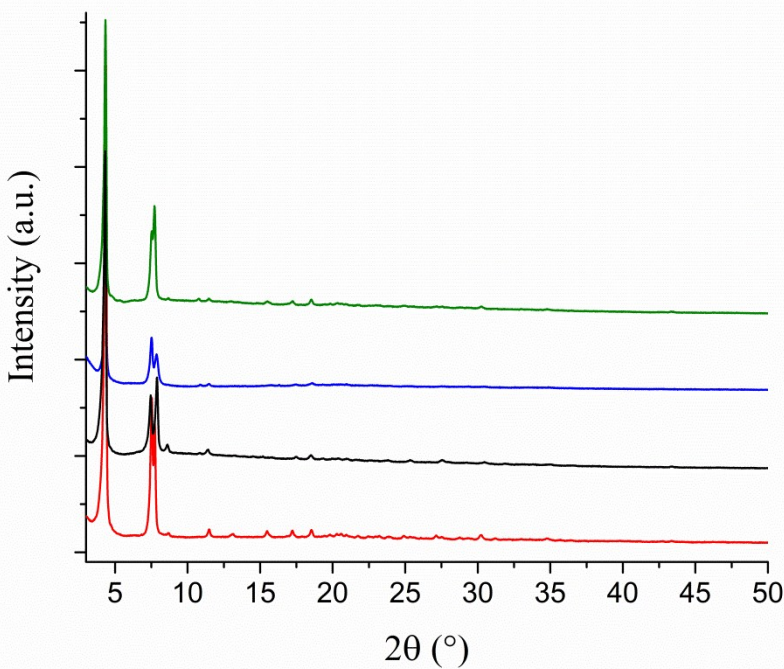


Fig. S12 XRPD patterns of **Cu(I)[CFA-4]** (blue curve), **K[CFA-4]** (red curve), **Ca(0.5)[CFA-4]** (green curve) and **Cs[CFA-4]** (black curve).

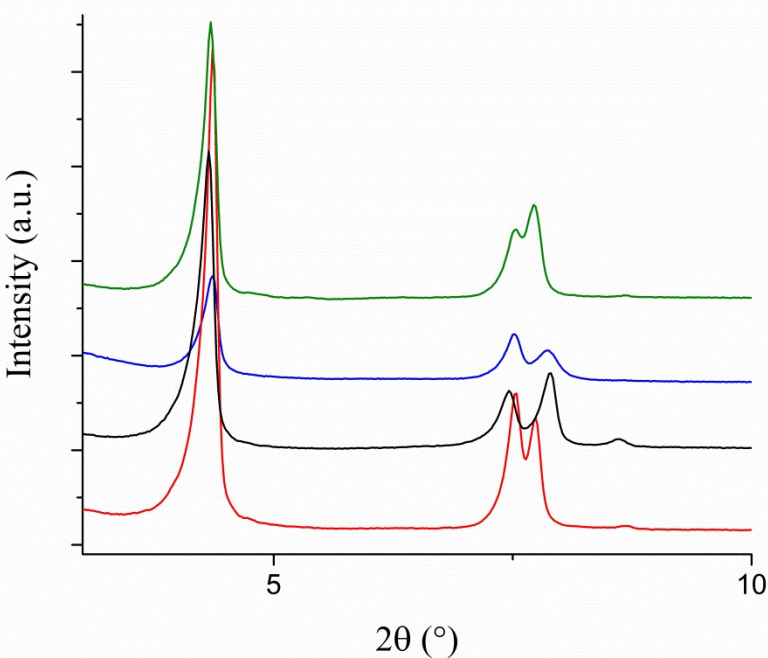


Fig. S13 XRPD patterns in the range $3\text{--}10^\circ$ 2θ of **Cu(I)[CFA-4]** (blue curve), **K[CFA-4]** (red curve), **Ca(0.5)[CFA-4]** (green curve) and **Cs[CFA-4]** (black curve).

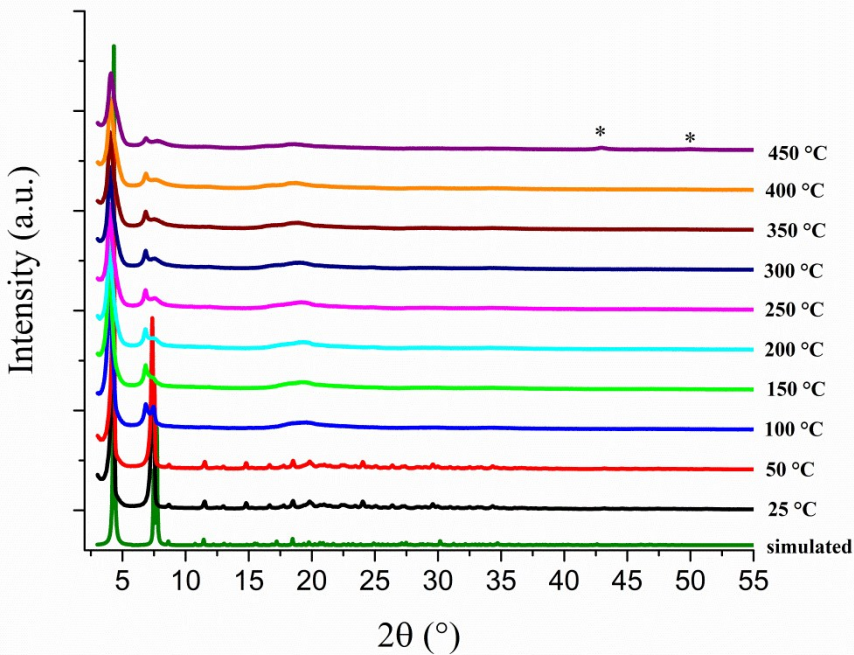


Fig. S14 VTXRPD plots of $\text{Cu}(\text{I})[\text{Cu}_5(\text{tfpb})_3] \cdot x\text{CH}_3\text{CN}$ in the range of 25-450°C. The first XRPD pattern is simulated based on the single crystal X-ray data. *peaks belong to Cu phase (PDF no. 4-836).

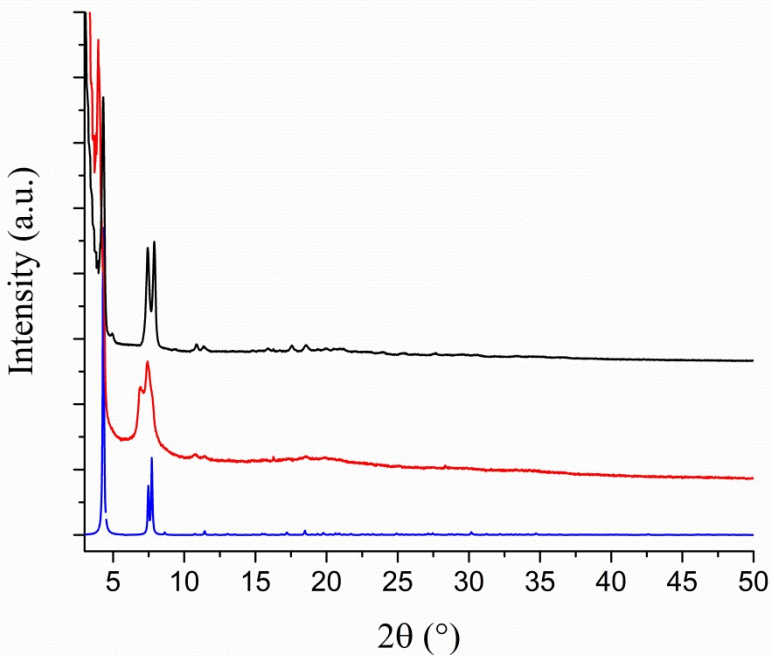


Fig. S15 XRPD patterns of simulated $\text{Cu}(\text{I})[\text{CFA-4}]$ (blue curve), oxidised $\text{Cu}(\text{I})[\text{CFA-4}]$ (red curve) and reduced $\text{Cu}(\text{I})[\text{CFA-4}]$ (black curve).

5. TGA curve

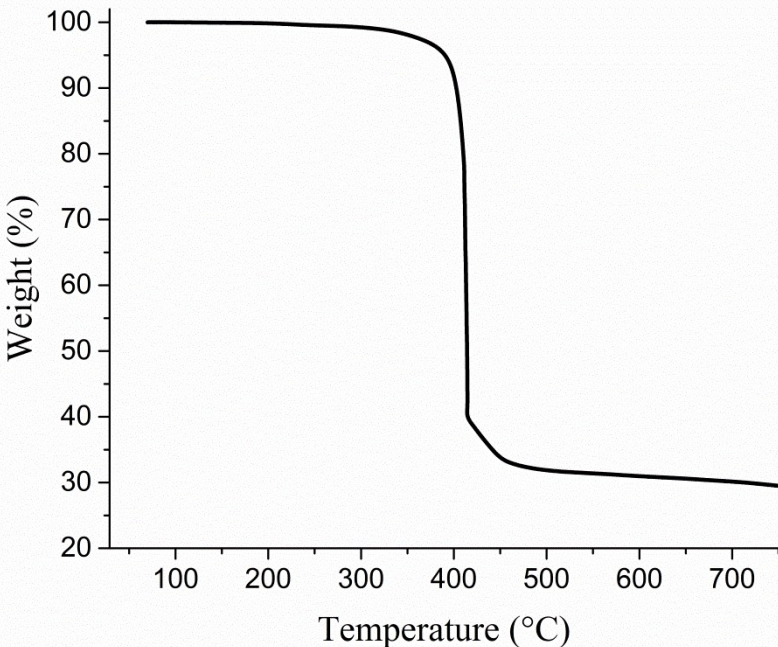


Fig. S16 Temperature dependent weight loss of **K[CFA-4]** under air.

6. Mass spectra

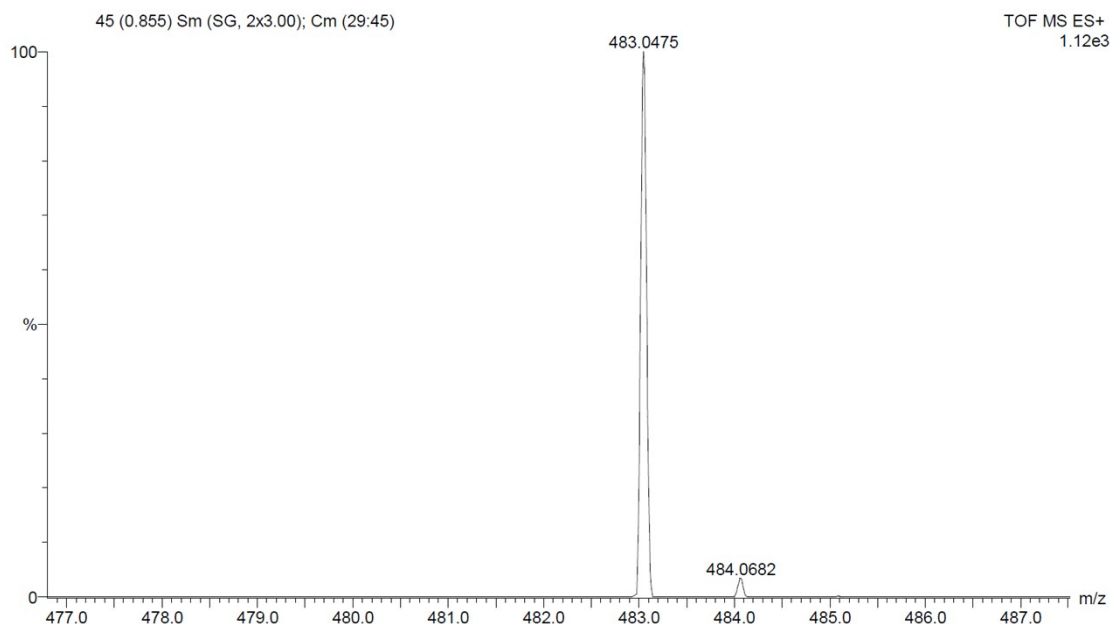


Fig. S17 Mass spectra of H₂-tfpb (TOF MS ESI+).

Table S2 Elemental Composition Report of H₂-tfpb.

Mass	Calc. Mass	mDa	PPM	DBE	Formula
483.0475	483.0478	-0.3	-0.5	-1.5	C ₈ H ₈ N ₄ F ₁₇
	483.0479	-0.4	-0.8	9.5	C ₁₆ H ₇ N ₄ F ₁₂
	483.0480	-0.5	-0.9	2.0	C ₁₃ H ₉ N F ₁₆
	483.0481	-0.6	-1.2	20.5	C ₂₄ H ₆ N ₄ F ₇
	483.0481	-0.6	-1.3	13.0	C ₂₁ H ₈ N F ₁₁
	483.0482	-0.7	-1.5	31.5	C ₃₂ H ₅ N ₄ F ₂
	483.0483	-0.8	-1.6	24.0	C ₂₉ H ₇ N F ₆
	483.0484	-0.9	-1.9	35.0	C ₃₇ H ₆ N F
	483.0422	5.3	11.1	31.5	C ₃₅ H ₆ F ₃
	483.0420	5.5	11.4	20.5	C ₂₇ H ₇ F ₈
	483.0420	5.5	11.5	28.0	C ₃₀ H ₅ N ₃ F ₄
	483.0419	5.6	11.6	35.5	C ₃₃ H ₃ N ₆
	483.0418	5.7	11.7	9.5	C ₁₉ H ₈ F ₁₃
	483.0418	5.7	11.8	17.0	C ₂₂ H ₆ N ₃ F ₉
	483.0418	5.7	11.9	24.5	C ₂₅ H ₄ N ₆ F ₅
	483.0417	5.8	12.0	-1.5	C ₁₁ H ₉ F ₁₈
	483.0416	5.9	12.1	6.0	C ₁₄ H ₇ N ₃ F ₁₄
	483.0416	5.9	12.2	13.5	C ₁₇ H ₅ N ₆ F ₁₀
	483.0414	6.1	12.5	2.5	C ₉ H ₆ N ₆ F ₁₅
	483.0540	-6.5	-13.5	2.0	C ₁₀ H ₈ N ₅ F ₁₅
	483.0542	-6.7	-13.8	13.0	C ₁₈ H ₇ N ₅ F ₁₀
	483.0542	-6.7	-13.9	5.5	C ₁₅ H ₉ N ₂ F ₁₄
	483.0543	-6.8	-14.2	24.0	C ₂₆ H ₆ N ₅ F ₅
	483.0544	-6.9	-14.2	16.5	C ₂₃ H ₈ N ₂ F ₉
	483.0545	-7.0	-14.5	35.0	C ₃₄ H ₅ N ₅
	483.0545	-7.0	-14.6	27.5	C ₃₁ H ₇ N ₂ F ₄
	483.0359	11.6	24.1	35.5	C ₃₆ H ₄ N ₂ F

Mass	Calc. Mass	mDa	PPM	DBE	Formula			
483.0357	11.8	24.4	24.5	C28	H5	N2	F6	
483.0357	11.8	24.5	32.0	C31	H3	N5	F2	
483.0355	12.0	24.8	13.5	C20	H6	N2	F11	
483.0355	12.0	24.9	21.0	C23	H4	N5	F7	
483.0354	12.1	25.1	2.5	C12	H7	N2	F16	
483.0353	12.2	25.2	10.0	C15	H5	N5	F12	
483.0352	12.3	25.5	-1.0	C7	H6	N5	F17	
483.0603	-12.8	-26.5	5.5	C12	H8	N6	F13	
483.0604	-12.9	-26.8	16.5	C20	H7	N6	F8	
483.0605	-13.0	-26.9	9.0	C17	H9	N3	F12	
483.0605	-13.0	-27.0	1.5	C14	H11		F16	
483.0606	-13.1	-27.1	27.5	C28	H6	N6	F3	
483.0606	-13.1	-27.2	20.0	C25	H8	N3	F7	
483.0607	-13.2	-27.3	12.5	C22	H10		F11	
483.0608	-13.3	-27.5	31.0	C33	H7	N3	F2	
483.0608	-13.3	-27.6	23.5	C30	H9		F6	
483.0610	-13.5	-28.0	34.5	C38	H8		F	
483.0296	17.9	37.1	32.0	C34	H4	N	F3	
483.0294	18.1	37.4	21.0	C26	H5	N	F8	
483.0294	18.1	37.5	28.5	C29	H3	N4	F4	
483.0293	18.2	37.7	10.0	C18	H6	N	F13	
483.0292	18.3	37.8	17.5	C21	H4	N4	F9	
483.0291	18.4	38.1	-1.0	C10	H7	N	F18	

7. EDX Data

Table S3 Cu/metal ratios for different M[CFA-4] samples, calculated from the data shown in Fig. S18-S20.

Sample	Copper/metal ratio
K[CFA-4]	5.12/1
Ca(0.5)[CFA-4]	10.76/1
Cs[CFA-4]	6.45/1

Elem	Wt %	At %	K-Ratio	Z	A	F
F K	30.04	57.38	0.1485	1.0734	0.4589	1.0034
K K	7.50	6.96	0.0686	1.0447	0.8700	1.0068
CuK	62.46	35.66	0.5911	0.9450	1.0014	1.0000
Total	100.00	100.00				

Element	Net Inte.	Backgrd	Inte. Error	P/B
F K	849.09	3.10	0.34	273.90
K K	325.87	0.12	0.55	2715.58
CuK	687.29	0.96	0.38	715.93

Fig. S18 EDX data for K[CFA-4].

Elem	Wt %	At %	K-Ratio	Z	A	F
F K	27.47	55.09	0.1436	1.0792	0.4825	1.0040
CaK	4.02	3.82	0.0396	1.0743	0.9051	1.0127
CuK	68.52	41.09	0.6530	0.9513	1.0019	1.0000
Total	100.00	100.00				

Element	Net Inte.	Backgrd	Inte. Error	P/B
F K	749.31	1.86	0.37	402.85
CaK	154.21	0.52	0.81	296.56
CuK	686.65	0.64	0.38	1072.89

Fig. S19 EDX data for Ca(0.5)[CFA-4].

Elem	Wt %	At %	K-Ratio	Z	A	F
CsL	24.50	13.43	0.2291	0.9017	1.0150	1.0215
CuK	75.50	86.57	0.7606	1.0339	0.9743	1.0000
Total	100.00	100.00				

Element	Net Inte.	Backgrd	Inte. Error	P/B
CsL	208.04	0.26	0.69	800.15
CuK	569.22	0.64	0.42	889.41

Fig. S20 EDX data for Cs[CFA-4].

8. Gas sorption measurements

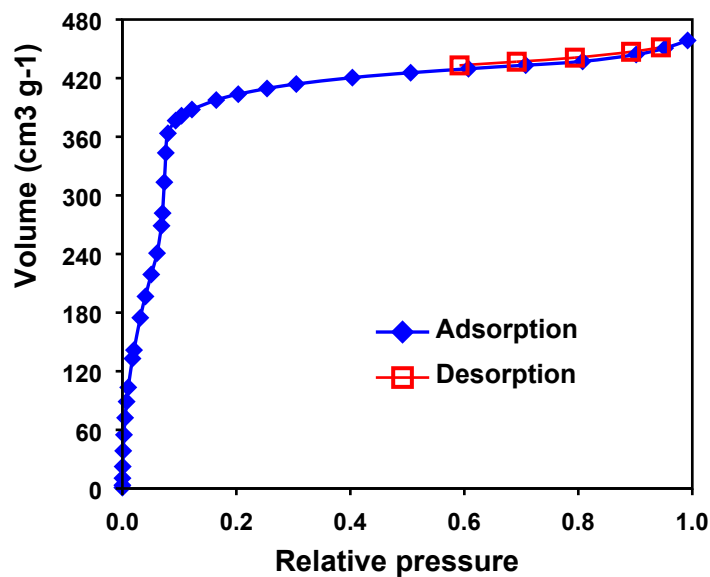


Fig. S21 Argon adsorption (blue) and desorption (red) isotherms at 87 K for **Cu(I)[CFA-4]** sample heated at 100 °C in vacuum.

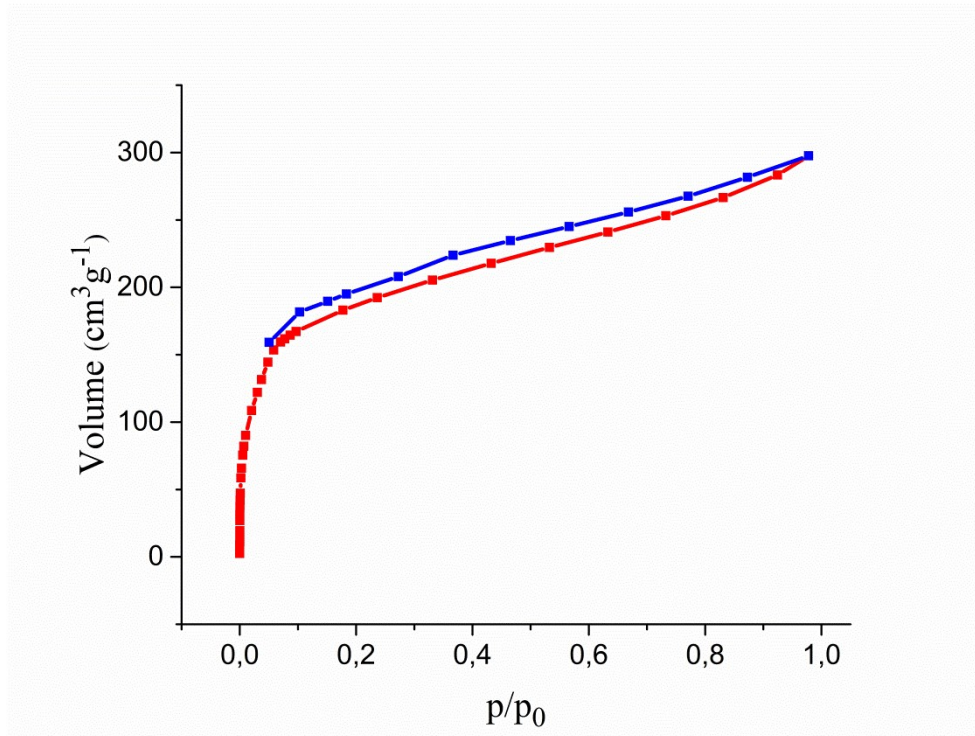


Fig. S22 Argon adsorption (red) and desorption (blue) isotherms at 77 K for **Cu(I)[CFA-4]** sample heated at 350 °C in vacuum.

The isosteric heats of adsorption were calculated from the measured isotherms (Figs. S23-25) using the Clausius-Clapeyron equation (**I**). The slopes of linear plots $\ln P$ versus $1/RT$ for different loadings (Fig. S26-28) give the adsorption enthalpies, according to the equation (**II**).

$$Q_{st} = -R \left(\frac{\partial(\ln P)}{\partial(1/T)} \right)_{\theta} \quad (\text{I}), \Theta - \text{surface coverage}$$

$$\ln P = -\frac{Q_{st}}{R} \left(\frac{1}{T} \right) + C \quad (\text{II}), C - \text{integration constant}$$

The isosteric heat of O_2 adsorption at zero limit surface coverage (initial heat of adsorption) has been determined using Henry's constants K_H , obtained as a slope from the linear ranges of isotherms at low pressure (Table S4 and Fig. S29). In this range the dependence of amount adsorbed (n) on pressure can be expressed with Henry's law (**III**). The initial isosteric heat of adsorption is obtained similarly using the Clausius-Clapeyron equation (**IV**) (Fig. S30).

$$n = K_H \cdot P \quad (\text{III})$$

$$\lim_{n \rightarrow 0} (Q_{st}) = Q_{st}^0 = R \left(\frac{\partial(\ln K_H)}{\partial(1/T)} \right) \quad (\text{IV})$$

Table S4. Henry's constants for O_2 adsorption on **CFA-4** ($\text{cm}^3 \text{ g}^{-1} \text{ kPa}^{-1}$)

T [K]	163	173	183
K_H	0.3971	0.2365	0.1534

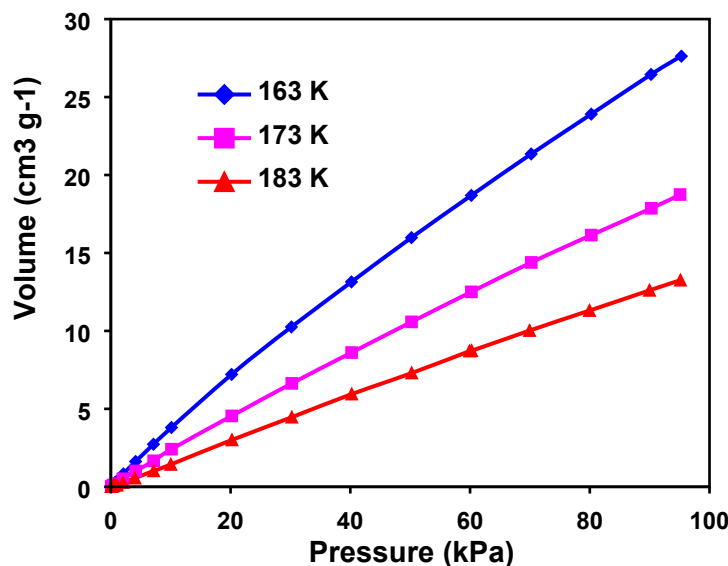


Fig. S23 O_2 adsorption isotherms for **Cu(I)[CFA-4]** at different temperatures.

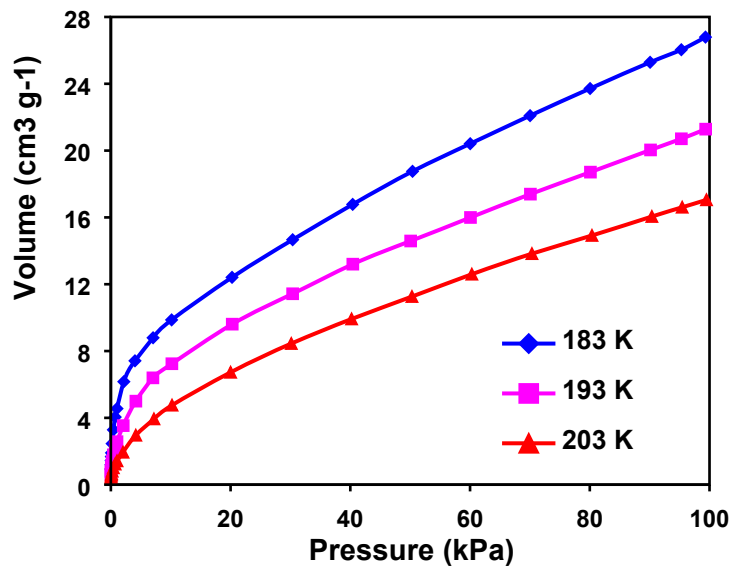


Fig. S24 CO adsorption isotherms for Cu(I)[CFA-4] at different temperatures.

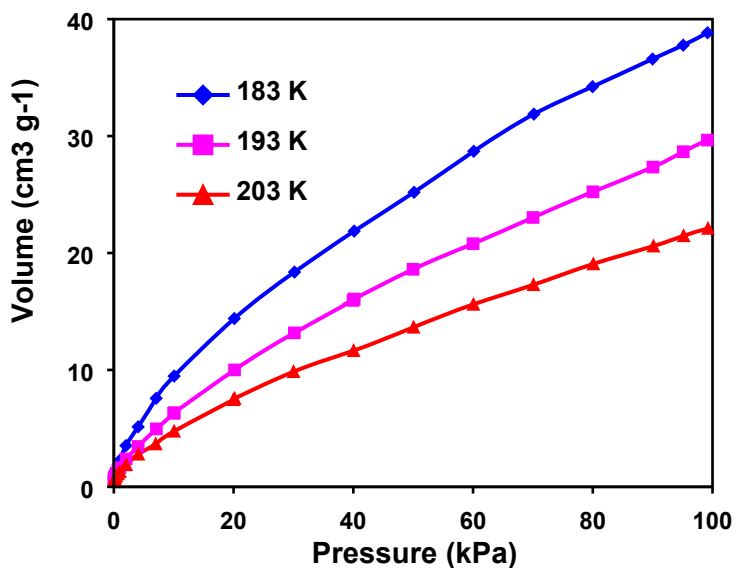


Fig. S25 CO adsorption isotherms for K[CFA-4] at different temperatures.

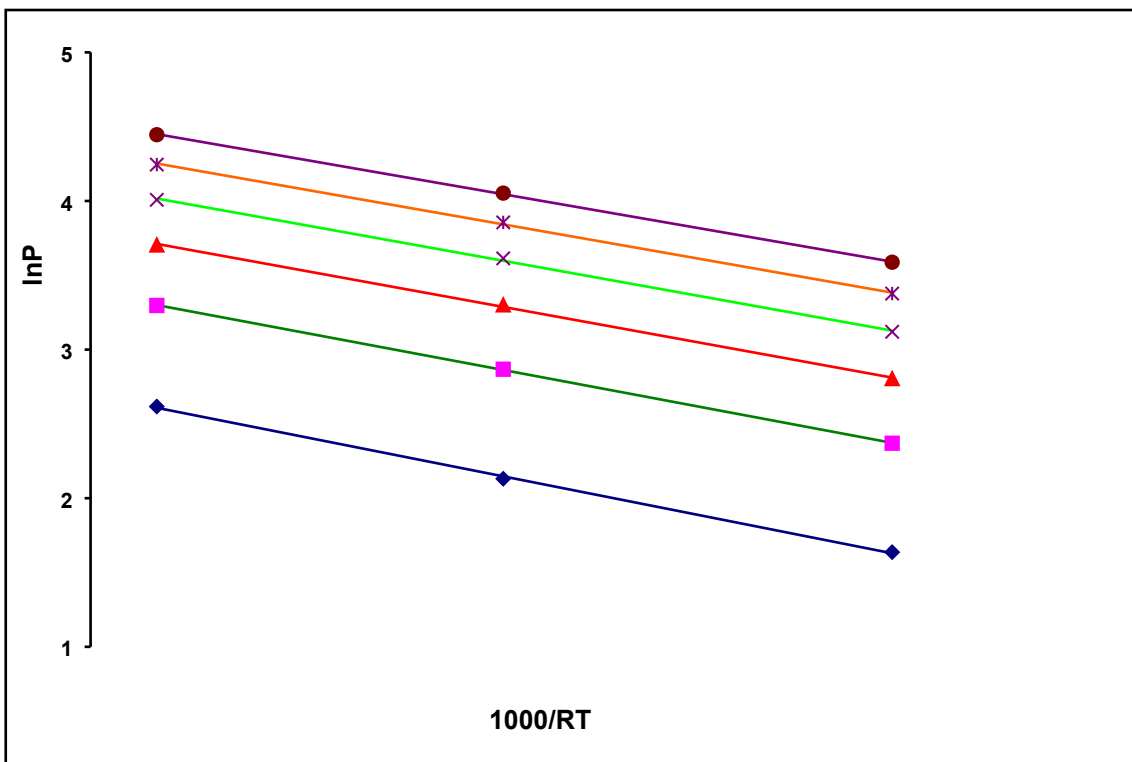


Fig. S26 $\ln P$ versus $1/RT$ plots for different loadings for O_2 adsorption on $\text{Cu}(\text{I})[\text{CFA}-4]$.

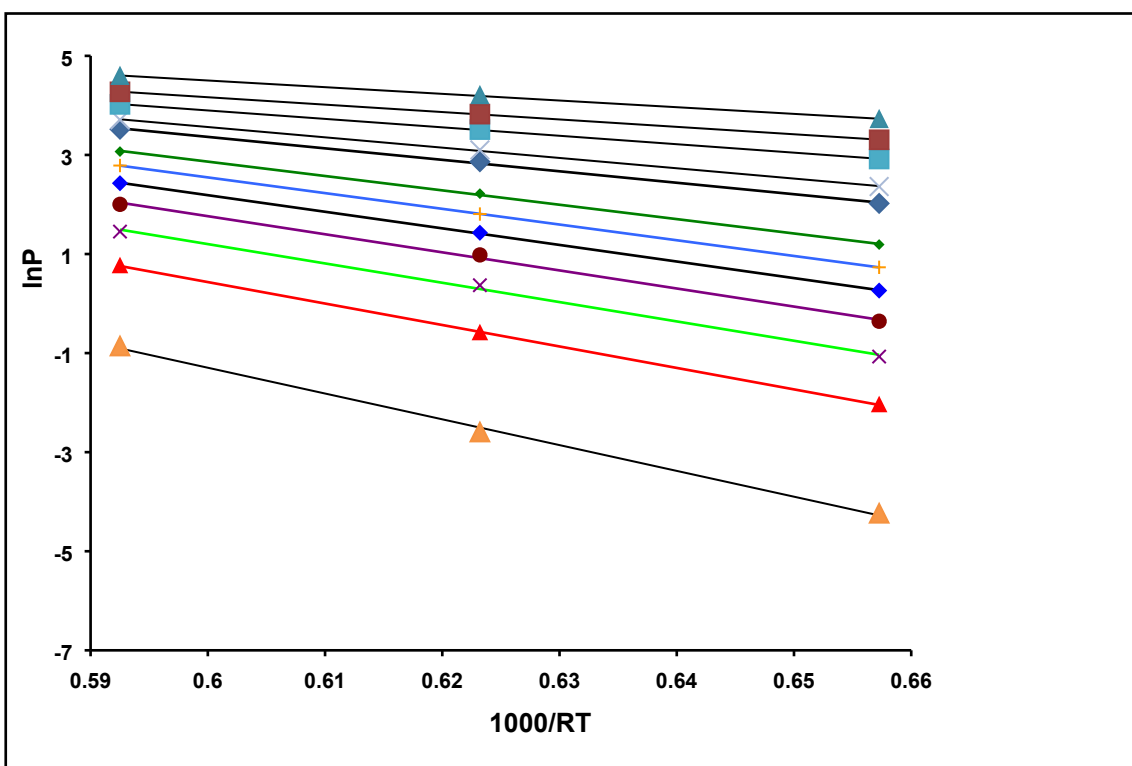


Fig. S27 $\ln P$ versus $1/RT$ plots for different loadings for CO adsorption on $\text{Cu}(\text{I})[\text{CFA}-4]$.

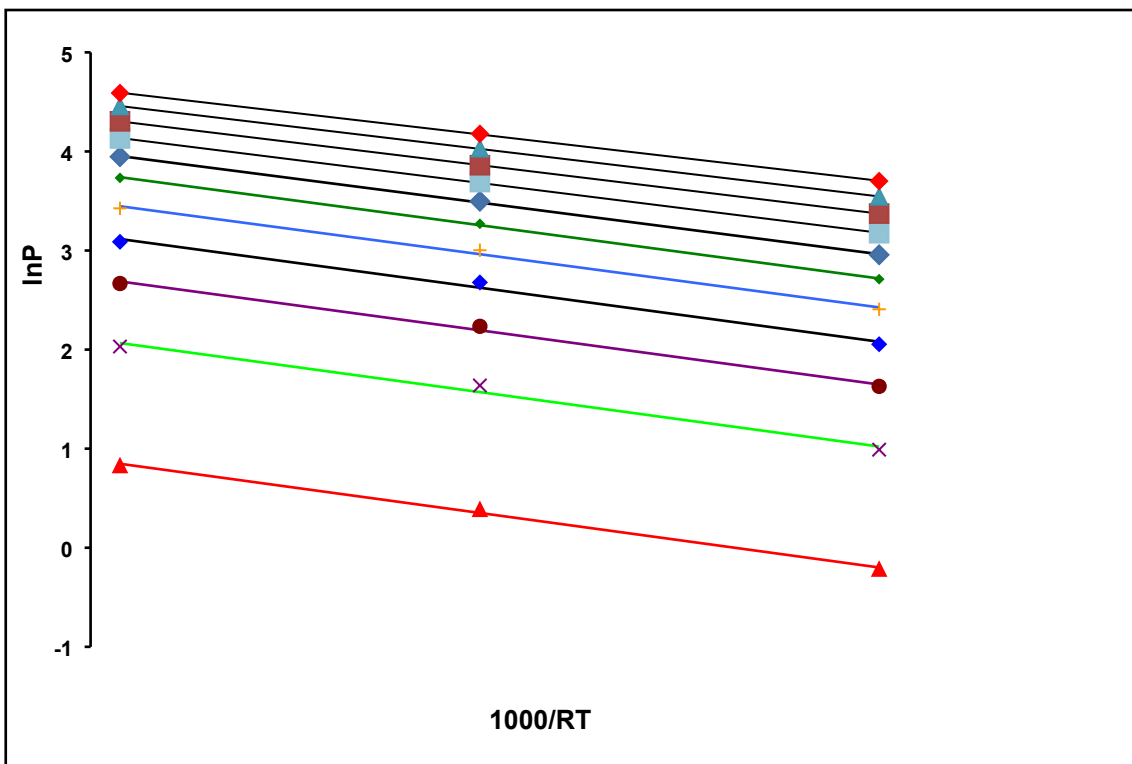


Fig. S28 $\ln P$ versus $1/RT$ plots for different loadings for CO adsorption on **K[CFA-4]**.

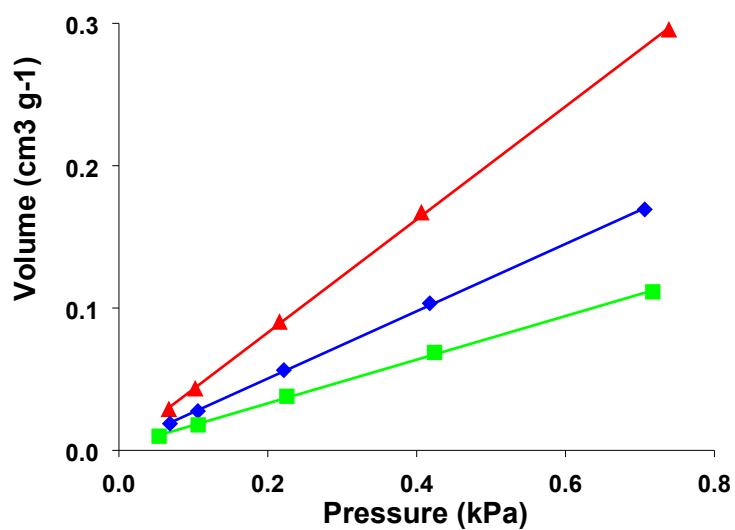


Fig. S29 Determination of Henry's constants for O_2 adsorption on **Cu(I)[CFA-4]**.

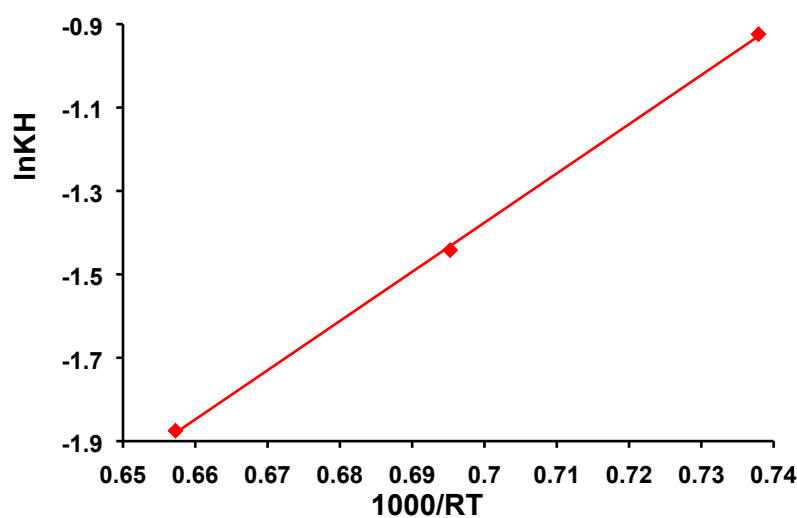


Fig. S30 $\ln K_H$ versus $1/RT$ plot for O_2 adsorption on $Cu(I)[CFA-4]$.

9. UV-Vis spectrum

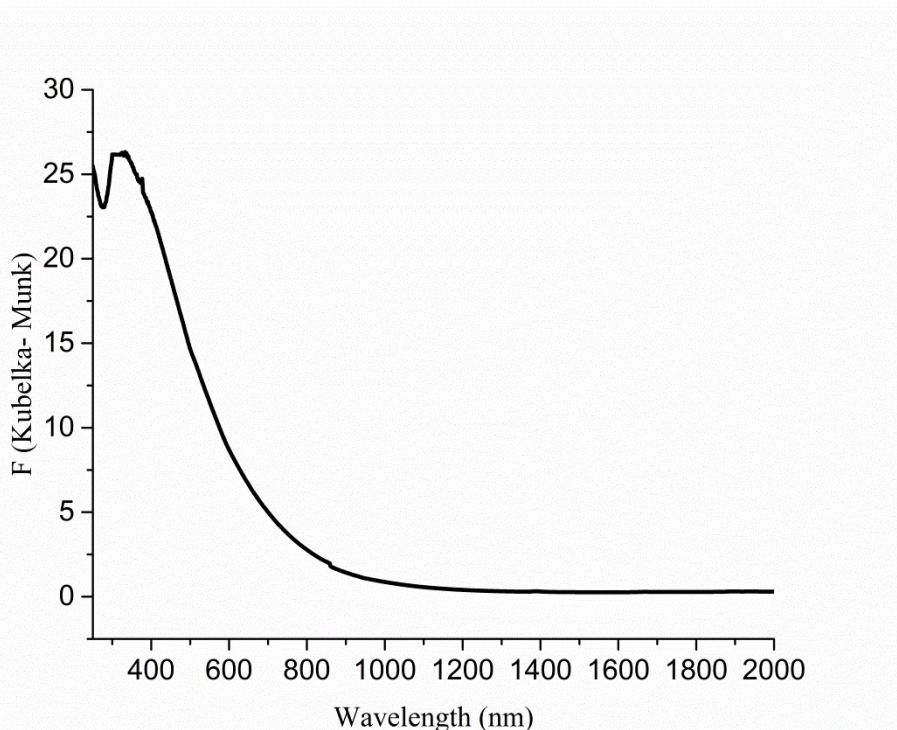


Fig. S31 UV-Vis spectrum of Cu(I)[CFA-4].

10. Photoluminescence spectra

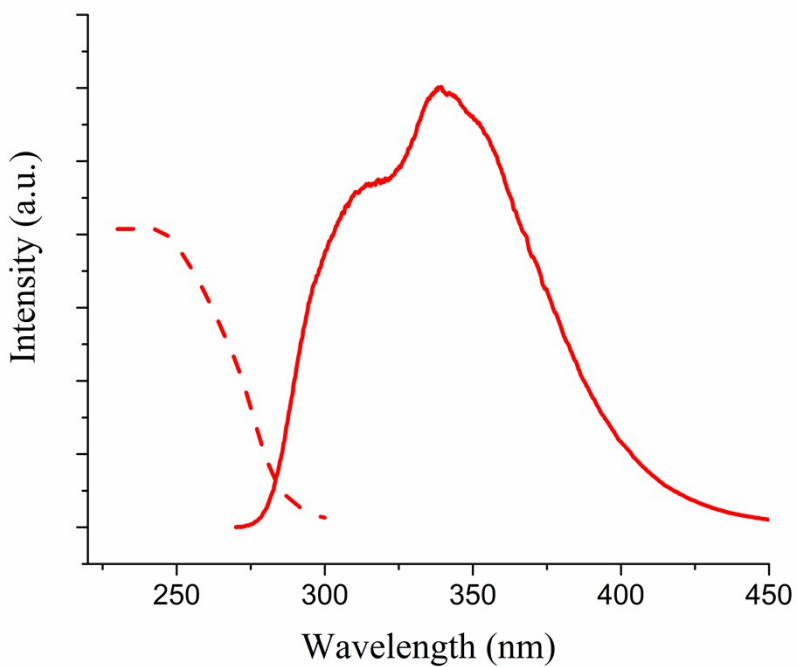


Fig. S32 Photoluminescence spectra of **1** at room temperature. Dashed line: excitation spectrum ($\lambda_{\text{em}} = 312 \text{ nm}$); Continuous line: emission spectrum ($\lambda_{\text{ex}} = 245 \text{ nm}$).

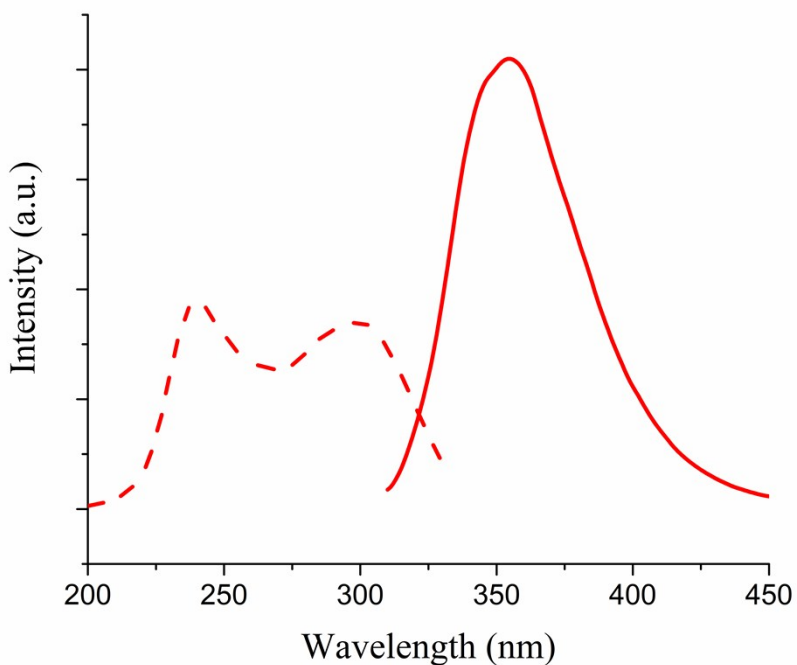


Fig. S33 Solid-state photoluminescence spectra for **1** at room temperature. Dashed line: excitation spectrum ($\lambda_{\text{em}} = 350 \text{ nm}$); Continuous line: emission spectrum ($\lambda_{\text{ex}} = 290 \text{ nm}$).

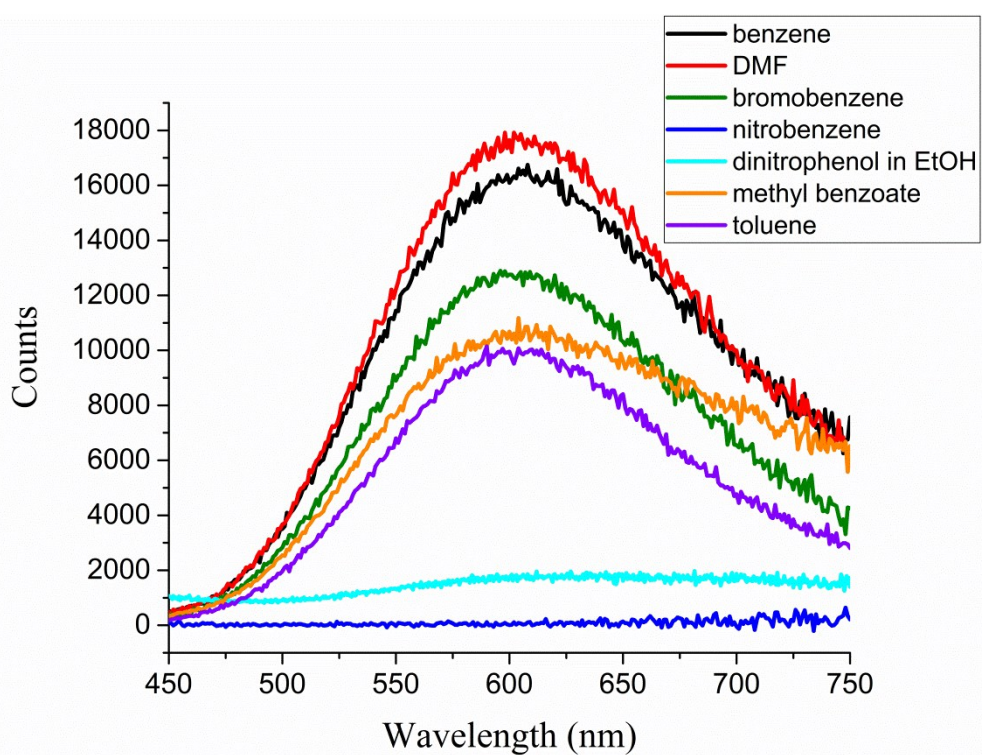


Fig. S34 Photoluminescence spectra of Cu(I)[CFA-4] at room temperature with different solvents (excitation wavelength 320 nm).